NJC

ROYAL SOCIETY OF CHEMISTRY

PAPER

View Article Online
View Journal

Check for updates

Cite this: DOI: 10.1039/d1nj00189b

Synthesis of a light-harvesting ruthenium porphyrin complex substituted with BODIPY units. Implications for visible light-promoted catalytic oxidations†

Jonathan Malone, Seth Klaine, Christian Alcantar, Fox Bratcher and Rui Zhang *

Received 12th January 2021,
Accepted 22nd February 2021

DOI: 10.1039/d1nj00189b

rsc.li/njc

A light-harvesting ruthenium porphyrin substituted covalently with four boron–dipyrrin (BODIPY) moieties has been synthesized and studied. The resulting complex showed an efficient decarbonylation reaction predominantly due to a photo-induced energy transfer process. Chemical oxidation of the ruthenium(II) BODIPY–porphyrin afforded a high-energy *trans*-dioxoruthenium(VI) species that is one order of magnitude more reactive towards alkene oxidation than those analogues supported by conventional porphyrins. In the presence of visible light, the ruthenium(II) BODIPY–porphyrin displayed remarkable catalytic activity toward sulfide oxidation and alkene epoxidation using iodobenzene diacetate [PhI(OAc)$_2$] and 2,6-dichloropyridine *N*-oxide (Cl$_2$pyNO) as terminal oxidants, respectively. The findings in this work highlight that porphyrin–BODIPY conjugated metal complexes are potentially useful for visible light-promoted catalytic oxidations.

Introduction

Catalytic oxidation of organic compounds is one of the most significant transformations in the large-scale production of many fine chemicals, pharmaceuticals, and commercial commodities.[1–3] Catalytic oxidation also plays an increasingly important role in both energy generation and conservation.[4,5] In nature, the ubiquitous cytochrome P450 enzymes (P450s) contain an iron porphyrin core and catalyze a wide variety of oxidation reactions with exceptionally high reactivity and selectivity, even so far as being able to functionalize inactivated hydrocarbons (paraffins).[6,7] In the pursuit of controllable and efficient oxidation catalysis, many synthetic metal complexes such as metalloporphyrins have been largely synthesized as enzyme-like oxidation catalysts for a variety of catalytic transformations.[8–11] In many enzymatic and synthetic oxidations, the metal catalyst is oxidized by a sacrificial oxidant to a high-valent metal–oxo species, which serves as oxygen atom transfer (OAT) species and then oxidizes the substrate.[12,13] In this context, ruthenium porphyrin complexes are among the most extensively studied biomimetic oxidation catalysts owing to their rich coordination, redox chemistry, and periodic relationship to the biologically significant metal iron.[9,14] Various sacrificial oxygen sources such as iodosylbenzene (PhIO), *tert*-butyl hydrogen peroxide (TBHP) and *m*-chloroperoxybenzoic acid (*m*CPBA) or periodate (IO_4^-) are associated with ruthenium porphyrins to catalyze epoxidation, hydroxylation, and oxidation of amines, and alcohols.[10,15] Notably, ruthenium porphyrin complexes display high regio-, chemo- and stereoselectivity in the catalytic oxidation of a variety of hydrocarbons with heteroaromatic *N*-oxides as oxygen source.[16–19] In addition, the well-characterized *trans*-dioxoruthenium(VI) porphyrin complexes have shown good reactivity toward organic substrates and catalyzed aerobic epoxidation of olefins in the absence of a reductant.[20–23]

As the demand for sustainable chemistry and environmentally friendly chemical processes increases, the use of visible light (sunlight) with a bioinspired photocatalyst offers an ideal way to harness solar energy in applied synthesis.[24–27] Our research group previously showed that in the presence of visible light ruthenium(II) carbonyl porphyrin complexes, abbreviated as [Ru^{II}(Por)(CO)], efficiently catalyze sulfoxidation with iodobenzene diacetate [PhI(OAc)$_2$] as a mild oxygen source.[28] The observed photo-promoted activity was ascribed to visible light photolysis of the carbonyl precursor to afford the ruthenium(II) decarbonylated species [Ru^{II}(Por)] that is more active for the generation of the OAT species in the catalytic cycle. With the aim of expanding the absorption region and harvesting the more available solar light, we initiated a study on exploring *core-antenna* systems that contain both boron–dipyrrin (BODIPY) dyes and metalloporphyrin units on the same molecule (Fig. 1). This supramolecular approach resembles photosynthetic organisms that use "antenna"-chromophore proteins to transfer absorbed light energy to the reaction center.[29] Such excited-energy transfer (EET)

Department of Chemistry, Western Kentucky University, 1906 College Heights Blvd #11079, Bowling Green, KY 42101-1079, USA. E-mail: rui.zhang@wku.edu; Fax: +1-270-745-55361; Tel: +1-270-745-3803

† Electronic supplementary information (ESI) available: Characterization spectra of compounds **1–3**. See DOI: 10.1039/d1nj00189b

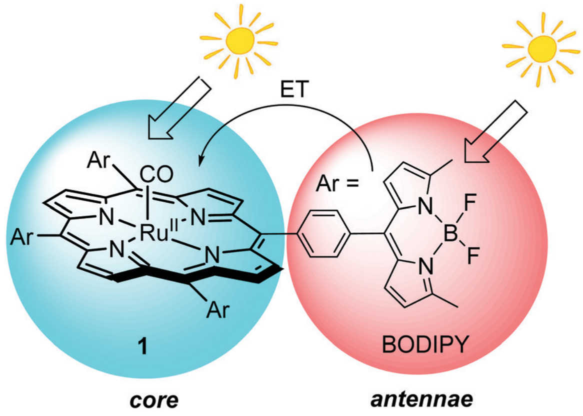

Fig. 1 Structure of porphyrin–BODIPY complex [Ru^{II}(L-Por)(CO)] and visible light-induced energy transfer (ET) process.

between different entities of matching energy is therefore of paramount importance to utilize the light energy in a wide spectral region.[30–32] For the antennae system, BODIPY dyes are highly desirable in view of their excellent photo-stability, high absorption coefficients, and high fluorescence quantum yields.[33–35] Thus, many BODIPY derivatives have been incorporated as energy donors with porphyrin or metalloporphyrin acceptors.[34,36–40] Herein, we report the preparation and studies of a new ruthenium(II) carbonyl complex supported by the BODIPY–porphyrin scaffold, denoted here as [Ru^{II}(L-Por)(CO)] (**1**). As a result, covalently combining two chromophore architectures of BODIPY–porphyrin in ruthenium complex (**1**) have separately exhibited predominantly visible light-induced excited-energy transfer process that resulted in a highly efficient decarbonylation reaction, the formation of a high energy *trans*-dioxoruthenium(VI) species as well as the remarkable light accelerating effect on catalytic sulfide and alkene oxidations. To the best of our knowledge, linked BODIPY–ruthenium porphyrin conjugates as potential oxidation photocatalysts have not been reported thus far.

Experimental section

Materials and instrumentation

All commercial reagents were of the best available purity and were used as supplied unless otherwise specified. Solvents including acetonitrile, methanol, chloroform, methylene chloride and 1,2,4-trichlorobenzene were purchased from Aldrich Chemical Co. and used as received. Boron trifluoride diethyl etherate ($BF_3{\cdot}OEt_2$), chloroform-d, 2,3-dichloro-5,6-dicyano-1,4-benzoquinone (DDQ), diisobutylaluminum hydride (DIBAL-H), iodobenzene diacetate [$PhI(OAc)_2$], trifluoroacetic acid (TFA), triruthenium dodecacarbonyl [$Ru_3(CO)_{12}$], and *p*-formylbenzonitrile were also obtained through Aldrich Chemical Co. and used as provided. All organic sulfide and alkene substrates for catalytic oxidations were passed through a dry column of active alumina (Grade I) before use. Pyrrole and 2-methylpyrrole were purchased from Aldrich Chemical Co. and was freshly distilled prior to use for synthesis. The corresponding ruthenium(II) carbonyl complex [Ru^{II}(L-Por)(CO)] (**1**) used for catalytic sulfoxidation and epoxidation were synthesized from modification of literature methods and characterized by NMR, IR, UV-vis spectroscopies and ESI-MS.

UV-vis spectra were recorded on an Agilent 8453 diode array spectrophotometer and fluorescence spectra were recorded on a PerkinElmer LS-55 spectrometer. IR spectra were acquired on a Bio-Rad FT-IR spectrometer, and ^{1}H NMR spectra were obtained on a JEOL ECA-500 MHz spectrometer at 298 K with tetramethylsilane (TMS) as the internal standard. Chemical shifts (ppm) are reported relative to TMS. Gas chromatograph analyses were conducted on an Agilent GC6890-MS5973 equipped with a flame ionization detector (FID) using a DB-5 capillary column. The above GC/MS system is also coupled with an auto sample injector. Reactions of [Ru^{II}(L-Por)(CO)] with excess of $PhI(OAc)_2$ were conducted in a chloroform solution at 23 ± 2 °C. Electrospray ionization-mass spectroscopy (ESI-MS) data was collected using an Agilent 500 LCMS ion trap system. Kinetic measurements were performed on an Agilent 8454 diode array spectrophotometer using standard 1.0 cm quartz cuvettes. Visible light was produced from a SOLA SE II light engine (Lumencor) configured with a liquid light guide (6–120 W) or from a Rayonet photo-reactor (RPR-100) with tungsten lamps (RPR-4190, 60–300 W).

Synthesis and characterization of BODIPY–porphyrin derivatives

4,4-Difluoro-3,5-dimethyl-8-(4-formylphenyl)-4-bora-3*a*,4*a*-diaza-*s*-indacene (2). Following a previously published procedure,[41] a solution of a dipyrromethane benzaldehyde derivative (1.85 g, 6.65 mmol) in CH_2Cl_2 (50 mL) was treated with DDQ (1.66 g, 7.3 mmol) and stirred for 1.5 h. A dark red solid precipitated from the solution. The solution was treated with triethylamine (4.64 mL, 33.3 mmol) allowing the precipitate to dissolve followed by the addition of $BF_3{\cdot}OEt_2$ (4.10 mL, 33.3 mmol). After stirring for an additional 2 h the reaction mixture was filtered through a long silica column (CH_2Cl_2) to give **2** as a brick red solid (0.73 g, 33.3%). ^{1}H-NMR (500 MHz, $CDCl_3$): δ_H, ppm: 10.11 (s, 1H, CHO), 8.00 (d, 2H, Ar–H, J = 8.08 Hz), 7.67 (d, 2H, Ar–H, J = 7.65 Hz), 6.64 (d, 2H, β-pyrrole, J = 3.84 Hz), 6.29 (d, 2H, β-pyrrole, J = 4.25 Hz), 2.65 (s, 6H, CH_3); UV-vis (CH_2Cl_2) λ_{max}: 330, 515 nm.

5,10,15,20-Tetrakis-(4,4-difluoro-3,5-dimethyl-4-bora-3*a*,4*a*-diaza-*s*-indacene phenyl)porphyrin [H_2(L-Por)] (3). The *meso*-substituted light-harvesting porphyrin ligand **3** was synthesized according to the reported procedure by Adler *et al.*[42] Freshly distilled pyrrole (80 μL, 1.15 mmol) and the BODIPY derived benzaldehyde **2** (400 mg, 1.15 mmol) were refluxed in a solution of propionic acid (10 mL). Recrystallization was conducted by allowing the solution to slow cool to ambient temperature and then submerging the flask into an ice bath. The precipitate was collected and washed thoroughly with methanol (*ca.* 25 mL). Column chromatography (silica, CH_2Cl_2/hexanes = 1 : 1) afforded the vermillion red product **3** (100 mg, 23.4%). ^{1}H-NMR (500 MHz, $CDCl_3$): δ_H, ppm: 8.97 (s, 8H, β-pyrrole), 8.39 (d, 8H, Ar–H, J = 8.02 Hz), 7.96 (d, 8H, Ar–H, J = 8.00), 7.13 (d, 8H, β-pyrrole, J = 4.06 Hz), 6.45 (d, 8H, β-pyrrole, J = 4.10), 2.76 (s, 24H, CH_3), −2.69 (s, 2H, inner-H); ^{13}C-NMR (500 MHz, $CDCl_3$): δ_C, ppm: 158.1, 143.8, 142.2, 134.8, 134.5, 133.9, 130.6, 129.0, 119.9, 119.6, 31.0, 29.8, 15.2; UV-vis (CH_2Cl_2) λ_{max} ($\log \varepsilon$):

346, 420 (Soret, 4.23), 512 nm (4.01); ESI-MS: *m*/*z* (%): found 1487.3 (100%) for $[M + H]^+$.

Ruthenium(II) carbonyl BODIPY–porphyrin $[Ru^{II}(\text{L-Por})(CO)]$ (1). The free ligand **3** (40 mg) was heated in a solution of 1,2,4-trichlorobenzene to 100 °C in a 100 mL round bottom flask attached to a condenser. $Ru_3(CO)_{12}$ (40 mg) was carefully added to the mixture and the solution was heated to reflux at 220 °C. TLC with dichloromethane as the eluent was used to determine reaction completion by indicating no free ligand remained. An additional 20 min of reflux was allotted to ensure complete ruthenium insertion of the porphyrin ligand. An alumina column was used to remove excess 1,2,4-trichlorobenzene by flushing with excess hexane. CH_2Cl_2 was then used to elute the desired product which was then evaporated to dryness, affording desired complex **1** as a brick red solid (20 mg, 46%). ^{1}H-NMR (500 MHz, $CDCl_3$): δ_H, ppm: 8.80(s, 8H, β-pyrrole), 8.39 (d, 4H, Ar–H, J = 7.71 Hz), 8.30 (d, 4H, Ar–H, J = 7.58 Hz), 7.91 (dd, 8H, Ar–H, J = 7.58 Hz), 7.12 (d, 8H, β-pyrrole, J = 3.98 Hz), 6.44 (d, 8H, β-pyrrole, J = 4.07 Hz), 2.78 (s, 24H, CH_3);^{13}C-NMR (500 MHz, $CDCl_3$): δ_C, ppm: 158.1, 144.0, 142.3, 134.8, 134.4, 133.8, 133.6, 132.2, 130.6, 128.8, 121.4, 119.8, 15.1; UV-vis (CH_2Cl_2): λ_{max} (log ε): 410 (Soret, 4.05), 515 (4.16), 576 nm; IR: ν, cm^{-1}: 1936 (CO), 1010 (pyrrolic C–H).

Synthesis and kinetics of *trans*-dioxoruthenium(VI)–oxo porphyrin (4)

Following previously reported work,[28] $[Ru^{VI}(\text{L-Por})(O)_2]$ (**4**) was produced by chemical oxidation of precursors **1** with $PhI(OAc)_2$ (2.5 to 5 equiv.) as the sacrificial oxidant. The reaction was monitored by UV-vis spectroscopy. Reactions of resulting dioxo species with excess amounts of organic substrates were conducted in solutions at 23 ± 2 °C. The approximate concentrations of $[Ru^{VI}(\text{L-Por})(O)_2]$ were estimated by assuming 100% conversion of ruthenium(II) precursor in the oxidation reaction. The rates of the reactions which represent the rates of oxo group transfer from $[Ru^{VI}(\text{L-Por})(O)_2]$ to substrate were monitored by the decay of the Soret absorption band (λ_{max} = 422 nm) of the oxo-species. The kinetic traces at λ_{max} of 422 nm displayed good pseudo-first-order behavior for at least four half-lives, and the data was solved to give pseudo-first-order observed rate constants, k_{obs}. Plots of these values against the concentration of substrate were linear in all cases. The second-order rate constants for reactions of the oxo species with the organic substrates were solved according to eqn (1), where k_0 is a background rate constant found in the absence of added substrate, k_{ox} is the second-order rate constant for reaction with the substrate, and [Sub] is the concentration of substrate.

$$k_{obs} = k_0 + k_{ox}[\text{Sub}] \tag{1}$$

General procedure for photocatalytic sulfide and alkene oxidations

In general, the photocatalytic reactions were performed in a Rayonet photoreactor (RPR-100) with a wavelength range of 400–500 nm (max = 419 nm) from 300 W mercury lamps (RPR-4190 × 12). The photocatalytic sulfoxidations typically consisted of 0.2% mol catalyst loading in 2 mL of methanol containing 0.5 mmol sulfide. 1.5 equivalent of $PhI(OAc)_2$ (0.75 mmol) and water (4.5 μL) was added to the reaction solution before it was irradiated at 25 ± 2 °C. The photocatalytic alkene epoxidations were performed in CH_2Cl_2 (2 mL) at *ca.* 23 °C with 1.1 equiv. 2,6-dichloropyridine *N*-oxide (0.55 mmol), substrate (0.5 mmol), 0.1 mol% catalyst.

Aliquots of the reaction solution at constant time intervals were analyzed by GC/MS to determine the formed products and yields with an internal standard (trichlorobenzene). All reactions were run at least in duplicate, and the data reported in Tables 1 and 2 represent the average of these reactions. Monitoring reaction by UV-vis spectroscopy before and after reactions indicated that no significant degradation of ruthenium catalyst was found after 12 h photolysis except in 1,2-dichloroethane and toluene.

Results and discussion

Synthesis and characterization

Scheme 1 shows the synthetic path to the target porphyrin–BODIPY conjugate and its ruthenium complex. The synthetic details including the full characterization data and spectra of these compounds are given in the Experimental section and ESI.†

Following a modified 3-step procedure described by Dolphin *et al.*,[41] the BODIPY-appended benzaldehyde **2** was accordingly synthesized from the acid-catalyzed condensation of commercially available 2-methylpyrrole and *p*-formylbenzonitrile followed by a sequence of nitrile reduction, DDQ oxidation, and chelation in the presence of triethylamine (TEA) and boron trifluoride etherate ($BF_3{\cdot}OEt_2$). Acid-catalyzed condensation of **2** and pyrrole under reflux in propionic acid solution gave the vermillion red desired product **3**,[42] herein abbreviated as $H_2(\text{L-Por})$, in 23% yield. The conventional two-step Lindsey's procedure for porphyrin synthesis[43] was also attempted, resulting in a much lower yield (<5%). In its ^{1}H-NMR spectrum, a broad singlet signal of two inner protons at δ −2.69 ppm is characteristic for free porphyrin ligand (Fig. S2 in the ESI†). In the positive mode ESI-MS spectrum of **3**, there is a dominant cluster peak at *m*/*z* 1487 ascribable to $[M + H]^+$ (Fig. S4, ESI†).

To obtain the desired metallated complex, free ligand **3** was refluxed with $Ru_3(CO)_{12}$ in 1,2,4-trichlorobenzene as described in the early study,[23] leading to ruthenium(II) carbonyl complex (**1**) in 46% yield. As expected, the ruthenium(II) species is stabilized by the carbonyl ligand as a strong σ donor. After chromatographic purification, $[Ru^{II}(\text{L-Por})(CO)]$ was completely separated from other byproducts and obtained in >99% purity based on ^{1}H-NMR spectroscopy. Complete metal insertion reaction was also confirmed by the absence of the broad singlet signal of the porphyrin inner protons at δ_H = −2.69 ppm and appearance of the well-resolved doublet, doublet splitting of the aromatic hydrogens at δ = 8.30 and 8.39 ppm (see Fig. S5, ESI†). In addition, 13 different types of carbon atoms anticipated for complex **1** are evidenced in the ^{13}C-NMR spectrum (Fig. S6,

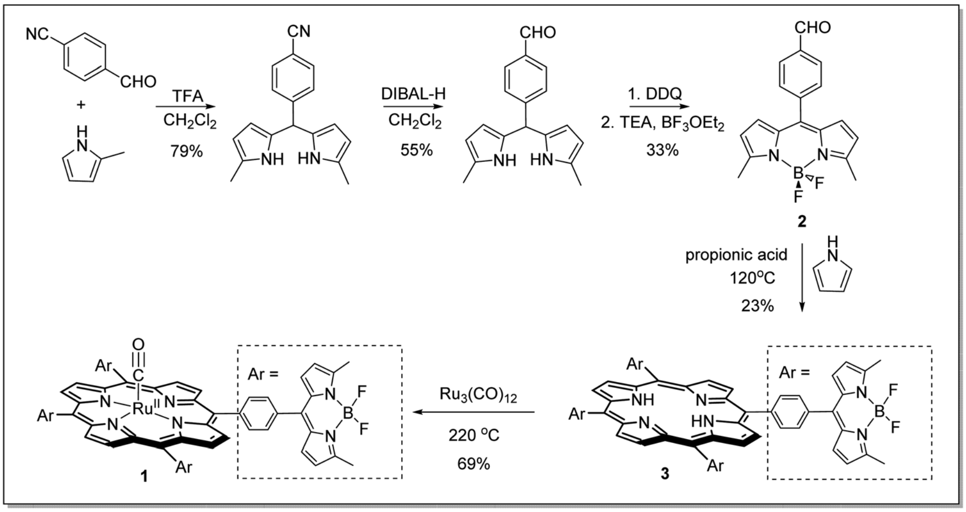

Scheme 1 Synthesis of porphyrin–BODIPY conjugated ligand and its ruthenium(II) complex **1**.

ESI†). The IR spectrum of **1** shows the characteristic stretch band for the carbonyl ligand at 1936 cm^{-1} and the unique oxidation state marker band resulted from rocking vibration of the pyrrole units at 1010 cm^{-1}, in agreement with a Ru^{II} formation[44] (see Fig. S7 in ESI†).

Photophysical properties

Fig. 2A shows the normalized absorption spectra of the porphyrin–BODIPY conjugate **3** together with the reference compounds BODIPY-appended benzaldehyde **2** and tetraphenyl porphyrin (H_2TPP), which was readily prepared according to Alder's reported method.[42] In CH_2Cl_2, the metal-free conjugate **3** showed two major absorption bands at 420 and 512 nm, suggesting that the combination of porphyrin and BODIPY architectures on **3** can efficiently extend the absorption region in the solar spectrum. Moreover, the absorption spectrum of **3** was essentially the same as the sum of the spectra of the two reference compounds **2** and H_2TPP. This spectral feature implied that there are no significant ground-state interactions between the chromophore components in BODIPY and porphyrin moieties. The insertion of ruthenium metal into the free BODIPY–porphyrin **3** is accompanied by a distinct color change from dark red to orange-red, and the UV-visible spectra in Fig. 2B showed that the Soret band of ruthenium(II) carbonyl porphyrin complex **1** is blue-shifted to 410 from 420 nm of BODIPY–porphyrin **3**, consistent with previously reported ruthenium(II) carbonyl complexes.[23]

The fluorescence spectra of **2** and **3** were measured by exciting both compounds at 515 nm. As shown in Fig. 3A, the emission spectrum of **2** exhibited a strong band at 540 nm, similar to previous studies.[45] The corresponding emission spectra of **3** showed only the band due to porphyrin at *ca.* 654 and 720 nm, but not the band attributable to BODIPY at *ca.*

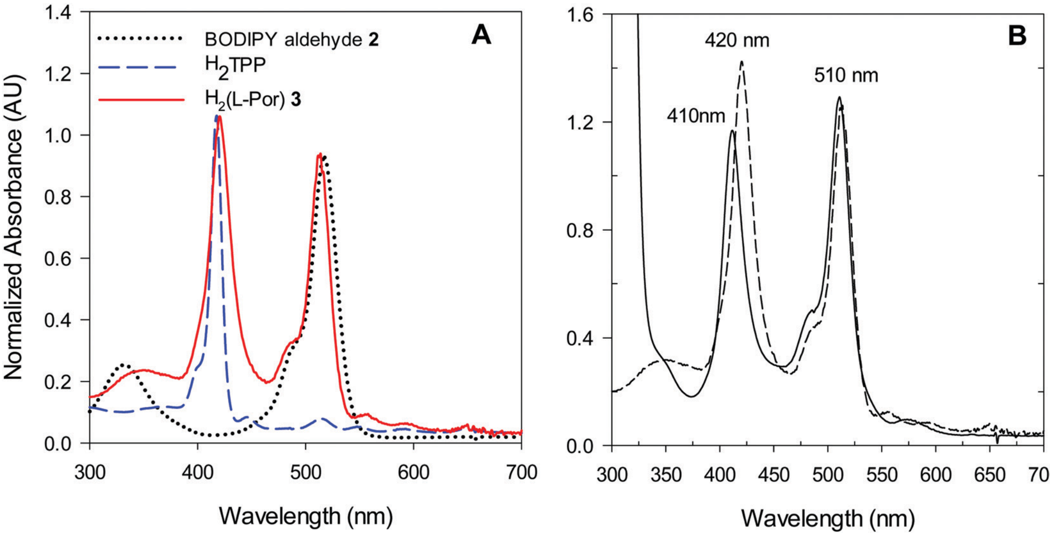

Fig. 2 (A) Normalized UV-vis spectra of **2** (dotted line), **3** (solid red line) and H_2TPP (dashed blue line) in CH_2Cl_2. The spectra of **2** and **3** were normalized at 512 nm and those of **3** and H_2TPP were normalized at 418 nm; (B) UV-vis spectra of $[Ru^{II}(L\text{-}Por)(CO)]$ **1** (solid line) and the free porphyrin–BODIPY ligand **3** (dashed line).

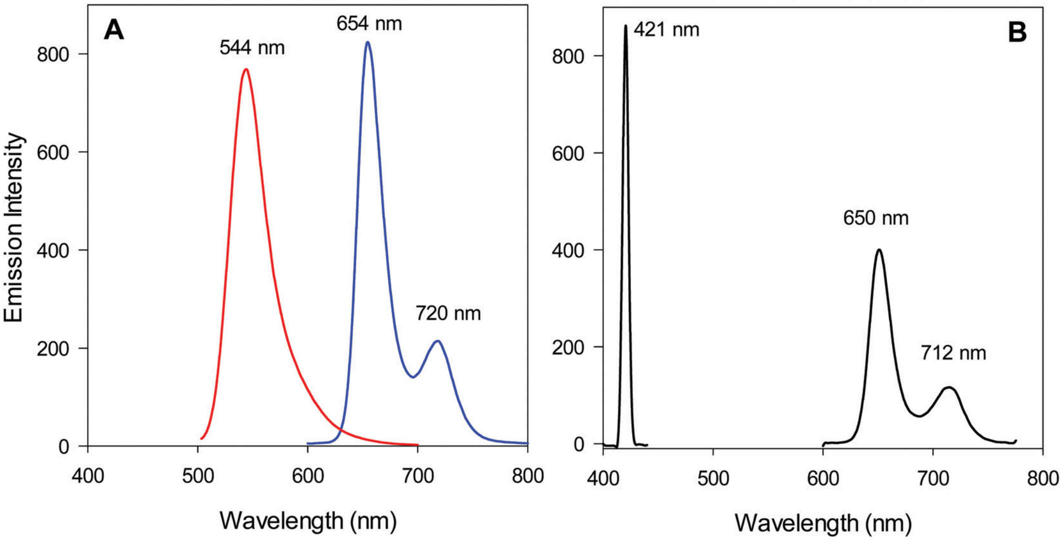

Fig. 3 (A) Fluorescence spectra of **2** (red) and **3** (blue) in CH_2Cl_2 at equal absorbance at 515 nm, both excited at 510 nm. (B) Fluorescence spectrum of **1** in CH_2Cl_2 excited at 419 nm.

540 nm. Similarly, the fluorescence spectrum of ruthenium complex **1** was also recorded by monitoring the porphyrin emission at 421, 650 and 712 nm (Fig. 3B), which closely resembled the emission of **3**. These observations suggested the presence of the energy transfer process in these BODIPY–porphyrin conjugates. According to the Förster mechanism,[46] the overlap between the fluorescence spectrum of BODIPY **2** and the absorption spectrum of porphyrin **3** at the Q band region (500–600 nm) apparently fulfilled the requirement for expected excited-energy transfer from energy donor BODIPY to energy acceptor porphyrin.[34] The plausible photo-induced electron transfer pathway between the excited BODIPY and porphyrin was not observed in this study.

Photochemical ejection of [Ru^{II}(L-Por)(CO)] (1)

In general, photo-induced decarbonylation (also termed photo-ejection) reactions are a common facet of ruthenium carbonyl complexes to afford a ruthenium(II), and therefore a more catalytically active form to react with different terminal oxidants.[28,47] In 2004, Ishii and coworkers demonstrated efficient photo-induced decarbonylation of a ruthenium(II) carbonyl octaethylporphyrin complex. The photochemistry was rationalized *via* a two-photon stepwise absorption process.[48] In this work, a highly efficient photo-ejection of the carbonyl ligand was observed under visible light irradiation from a SOLA light engine (output power 120 W). As shown in Fig. 4, compound **1** in CH_3CN proceeded with a rapid photo-ejection over 20 s upon visible light irradiation (120 W) instead of commonly required higher energy UV-light,[47] exhibiting a slightly red-shifted Soret band at 412 nm from 410 nm. For comparison, the photo-ejection of a conventional [Ru^{II}(TPP)(CO)] occurred at a much slower rate (*ca.* 450 s) under the same condition (data not shown here). The highly efficient photo-ejection reaction of the ruthenium complex **1** provided further evidence for a visible light-induced energy transfer process from the BODIPY–antennae to the ruthenium(II) carbonyl porphyrin center.

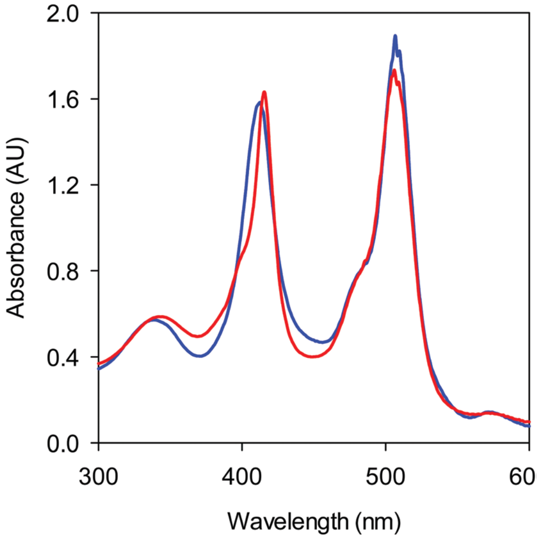

Fig. 4 UV-vis spectra change for photo-ejection of [Ru^{II}(L-Por)(CO)] (**1**) under visible light irradiation (120 W) in CH_3CN (blue spectrum at t = 0 and red spectrum at 20 s).

Generation of a *trans*-dioxoruthenium(VI) porphyrin [Ru^{VI}(L-Por)(O)$_2$]

Application of peroxyacids or other sacrificial oxidants to ruthenium(II) porphyrins have been shown to generate relatively stable *trans*-dioxoruthenium(VI) porphyrin complexes, which show good reactivity toward a variety of organic substrates including alkenes[49,50] In this study, subjecting complex **1** to PhI(OAc)$_2$ (*ca.* 5 eq.) in a solution of $CHCl_3$ also resulted in generation of a light-harvesting *trans*-dioxoruthenium(VI) compound **4**, *i.e.* [Ru^{VI}(L-Por)(O)$_2$]. The mild oxidant PhI(OAc)$_2$

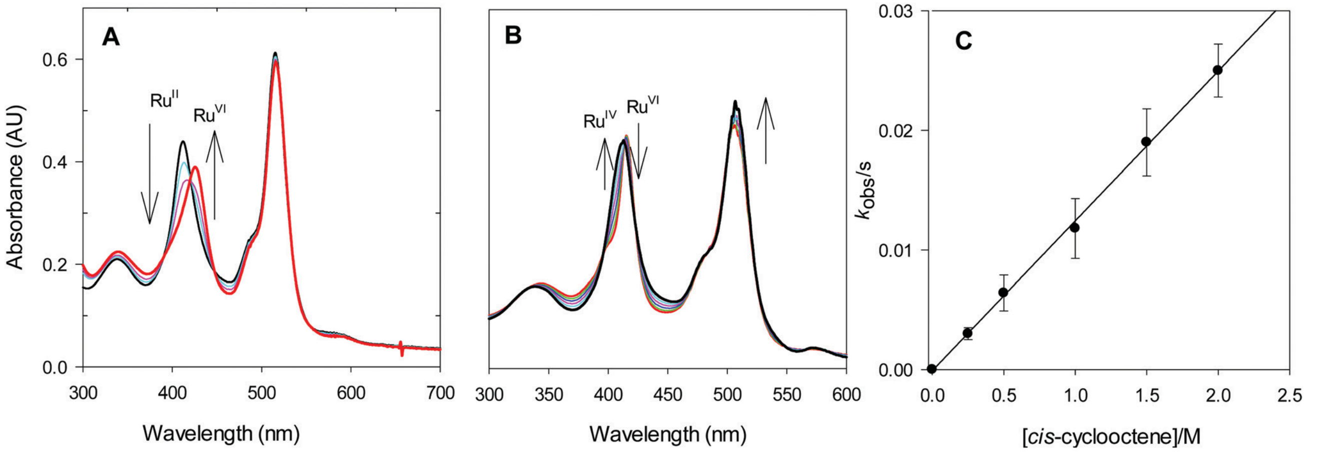

Fig. 5 (A) Time-resolved spectra for the chemical generation of [Ru^{VI}(L-Por)(O)$_2$] (**4**) following treatment of PhI(OAc)$_2$ (20 equiv.) to a solution of [Ru^{II}(L-Por)(CO)] (**1**) in CHCl$_3$ over 20 s. (B) Time-resolved spectra for the reaction of **4** in the presence of *cis*-cyclooctene (1 M) over 2 min. (C) Kinetic plot of observed rate constants for the reaction of **4** *versus* concentrations of *cis*-cyclooctene.

is advantageous for the generation and study of **4** because it neither decomposes the porphyrin complexes under usual conditions nor reacts with organic substrates.[28,51] The oxidation progress was monitored by UV-vis spectroscopy, and the representative time-resolved spectra in Fig. 5A showed the decay of the precursor **1** and growth of the oxo product **4** with clean isosbestic points over 20 s. Consequently, species **4** displayed a red-shifted Soret band at λ_{max} = 422 nm that is characteristic of the corresponding *trans*-dioxoruthenium(VI) porphyrins.[52,53] Of note, the redox process on the metal center showed a small impact on the change of the absorption band of the linked BODIPY moieties. In CH$_3$CN, generation of the [Ru^{VI}(L-Por)(O)$_2$] **4** occurred much more slowly than in CHCl$_3$ and required a longer time for completion (data not shown), suggesting a stabilizing effect exhibited by relatively coordinating CH$_3$CN on the [Ru^{II}(L-Por)(CO)] complex.[40] In both solutions, **4** gradually decayed back within several hours to the ruthenium(II) precursor as indicated by the UV-vis spectrum with a blue shifted, weaker absorption band at *ca.* 410 nm. Owing to its transient nature, **4** was not isolated and purified for further spectroscopic characterization.

As expected, complex **4** is reactive toward organic substrates such as *cis*-cyclooctene. When a solution of **4** and *cis*-cyclooctene in CHCl$_3$ was stirred at room temperature for a couple of minutes, *cis*-cyclooctene oxide was formed with over 90% yield. In the presence of visible light, oxo transfer from **4** to the alkene substrate gave a reduced ruthenium(IV) product (Fig. 5B) which has been known for decades.[52] The observed rate constants increased as the function of the substrate concentration, and the slope of the linear plot in Fig. 5C revealed a second-order rate constant of $k_{ox} = (1.2 \pm 0.1) \times 10^{-2}\ M^{-1}\ s^{-1}$ for the reaction of **4** with *cis*-cyclooctene. By comparison, the reactivity of **4** was at least 1 order of magnitude greater than those of the regular [Ru^{VI}(Por)](O)$_2$] ($k_{ox} = 10^{-4}$–$10^{-3}\ M^{-1}\ s^{-1}$) for the same substrate.[23] These findings suggest that the presence of energy transfer from the highly efficient light-harvesting BODIPY to the porphyrin metal center increased the potential energy of **4** in a significant way.

Photocatalytic oxidations by [Ru^{II}(L-Por)(CO)] (1)

The swift photo-ejection reaction of porphyrin–BODIPY conjugate **1** under visible light and the formation of high potential energy oxo species **4** prompted us to evaluate its photocatalytic potential in the oxidation of sulfides and alkenes. In light of the above photochemical investigations along with the previously reported work,[28] we anticipate that the porphyrin–BODIPY complex **1** could capture a broad spectrum of visible light using both antennae and core chromophores, and at the same time, exhibit a highly efficient energy transfer from the excited BODIPY antennae to the metalloporphyrin center for more efficient photo-induced catalytic transformations.

The catalytic oxidation of thioanisole was first investigated with **1** as the catalyst and PhI(OAc)$_2$ as the oxygen source. Our previous

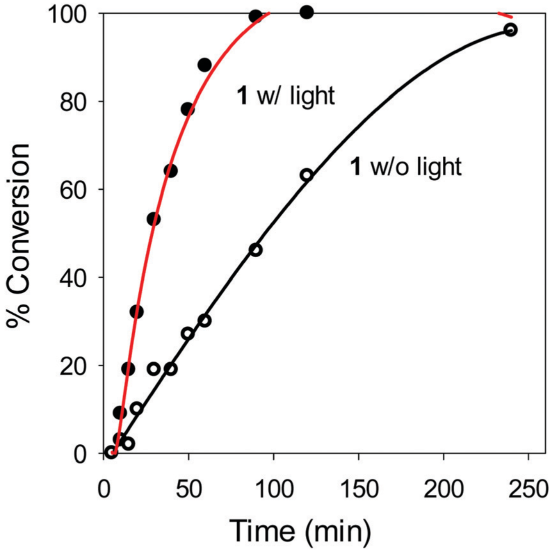

Fig. 6 Time courses of oxidation of thioanisole (0.5 mmol) with PhI(OAc)$_2$ (0.75 mmol) in CH$_3$OH (2 mL) at room temperature catalyzed by ruthenium(II) porphyrin **1** (1 μmol) in the presence of H$_2$O (4.5 μL) with visible light (red line with black circle) and without visible light (black line with white circle).

works have shown that $PhI(OAc)_2$ in the presence of a small amount of water was an efficient oxygen source for metalloporphyrin and metallocorrole-catalyzed oxidations.[28,51,54–56] Under established optimal conditions, our results collected in Fig. 6 and Table 1 show the light-harvesting complex **1** catalyzed efficient oxidation of thioanisoles to corresponding methyl phenyl sulfoxides in excellent yields and selectivities. Of note, a remarkable light acceleration effect was observed for all substrates. For example, complex **1** catalyzed the oxidation of thioanisole to the corresponding sulfoxide and 97% conversion was obtained after 4 h (Table 1, entry 1). Under visible light irradiation, the reaction proceeded more rapidly and 100% conversion was achieved within 1.5 h (entry 2). In comparison to our previous study,[28] the conventional [Ru^{II}(TMP)(CO)] (TMP = tetramestiylporphyrin) gave considerably lower activity, and only 10% conversion within 24 h in the absence of light (entry 3) and 94% conversion within 6 h with light (entry 4) were obtained, respectively.

Since ruthenium porphyrin complexes can efficiently catalyze the oxidation of hydrocarbons with pyridine *N*-oxides,[16,18] we also examined **1** as the potential photocatalyst towards the epoxidation of a variety of substituted styrenes with 2,6-dichloropyridine *N*-oxide under visible light irradiation (Table 2). Again, a remarkable light acceleration was observed in the catalytic alkene epoxidations. Treatment of styrene (0.5 mmol) with Cl_2pyNO (0.55 mmol) and **1** (0.5 μmol) in CH_2Cl_2 at room temperature afforded styrene oxide as the major product in 88% conversion within 6 h (Table 2, entry 1). In sharp contrast, when **1** was used as the catalyst in the absence of light conditions, the same transformation gave a sluggish reaction with <5% conversion (entry 2). When dichloroethane or toluene was used instead of CH_2Cl_2 for the catalytic styrene epoxidation, slightly reduced activities as well as significant catalyst degradation resulted (entries 3 and 4). Other substituted styrenes under the standard conditions underwent similar epoxidation to give their epoxides in over 90% selectivities albeit with appreciable lower conversions within the same time of period (Table 2, entries 5–8). Complex **1** was found to catalyze the *cis*-stilbene oxidation with complete stereoretention (>99% for *cis*-epoxide) and conversion of 38% was obtained (Table 2, entry 9). The oxidation of *cis*-cyclooctene was equally effective, affording the epoxide as the only product in 44% conversion (Table 2, entry 10). A series of control experiments indicated that no significant oxidized products were formed in the absence of either oxygen source nor catalyst **1**, or only in the presence of metal-free precursors **2** or **3**.

Table 1 Catalytic sulfoxidation of thioanisoles by Ru^{II}(L-Por)(CO)[a]

Entry	Substrate	Time (h)	Convn[b] (%)	Product	Selectivity[c]
1[d]	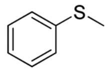	4	97	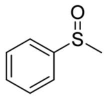	93 : 07
2		1.5	100		92 : 08
3[e]		24	10		99 : 01
4[f]		6	94		99 : 01
5	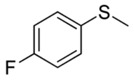	1	97	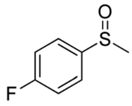	96 : 04
6	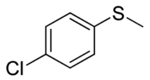	1	96	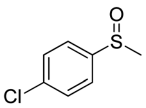	85 : 15
7	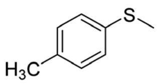	1.2	100	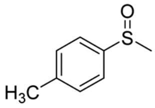	87 : 13
8	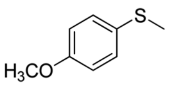	1.5	100	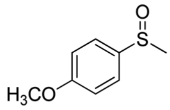	88 : 12
9	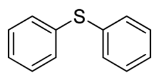	2	50	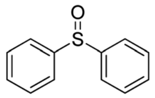	76 : 24

[a] All reactions were conducted with visible light irradiation (λ_{max} = 420 nm) in a Rayonet reactor or otherwise noted. All reactions were performed in CH_3OH (2 mL) at *ca.* 23 °C with 1.5 equiv. of $PhI(OAc)_2$ (0.75 mmol), substrate (0.5 mmol), 0.2 mol% catalyst in the presence of H_2O (4.5 μL); only sulfoxide and small amounts of sulfone were detected by GC-MS analysis of the crude reaction mixture. [b] Based on the conversion from substrate to products. [c] Ratio of products (sulfoxide : sulfone). [d] Without visible light irradiation. [e] [Ru^{II}(TMP)(CO)] as the catalyst without light irradiation from previously reported work.[28] [f] [Ru^{II}(TMP)(CO)] as the catalyst with light irradiation from previously reported work.[28]

Table 2 Catalytic epoxidation of styrenes by Ru^{II}(L-Por)(CO)[a]

Entry	Substrate	Time (h)	Conv.[b] (%)	Product	Selectivity[c]
1	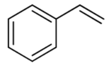	6	88	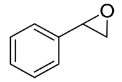	96 : 04
2[d]		6	<5		>99%
3[e]		3	56		98 : 02
4[f]		6	64		95 : 05
5	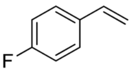	6	41	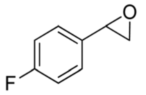	94 : 06
6	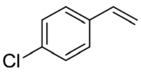	6	75	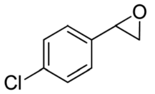	97 : 03
7	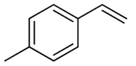	6	28	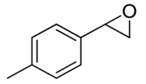	82 : 18
8	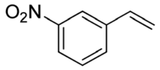	6	45	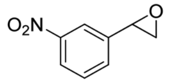	>99%
9	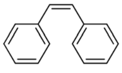	6	38	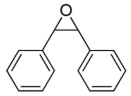	>99%
10	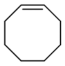	6	44	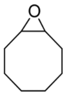	>99%

[a] All reactions were conducted with visible light irradiation (λ_{max} = 420 nm) in a Rayonet reactor or otherwise noted. All reactions were performed in CH_2Cl_2 (2 mL) at *ca.* 23 °C with 1.1 equiv. 2,6-dichloropyridine *N*-oxide (0.55 mmol), substrate (0.5 mmol), 0.1 mol% catalyst. [b] Based on the conversion of substrates. [c] Ratio of products (epoxide *vs.* other products). [d] Without visible light irradiation. [e] In 1,2-dichloroethane. [f] In toluene.

Conclusions

In conclusion, we have prepared and studied a novel light-harvesting BODIPY–porphyrin ligand and its corresponding carbonyl ruthenium(II) complex, which exhibits a broad absorption of visible light using both the porphyrin core and antennae chromophores. Under visible light irradiation, a highly efficient decarbonylation reaction of **1** and the formation of a more reactive *trans*-dioxoruthenium(VI) species were observed, indicating a photo-induced energy transfer from the BODIPY to the metalloporphyrin center. Notably, the ruthenium BODIPY–porphyrin complex has demonstrated a remarkable light acceleration effect on the selective sulfide oxidation and alkene epoxidation using PhI(OAc)$_2$ and Cl$_2$pyNO as terminal oxidants, respectively. The findings in this work suggest that porphyrin–BODIPY conjugated metal complexes are potentially useful for visible light-promoted catalytic oxidations. Further investigation of substrate scope, optimization of reaction conditions, other inexpensive and environmentally friendly oxygen sources, and their oxidation mechanisms are currently underway in our laboratory.

Author contributions

Conceptualization: R. Zhang. Investigation and experiments: J. Malone, S. Klaine, C. Alcantar and F. Bratcher: Writing-Original draft preparation: S. Klaine and R. Zhang. Writing-Reviewing and Editing; R. Zhang and all others contributed. Project administration: R. Zhang.

Conflicts of interest

There are no conflicts to declare.

Acknowledgements

This research is supported by the National Science Foundation (CHE1764315). S. Klaine, C. Alcantar and F. Bratcher are greatly thankful for internal grants (FUSE and GSRG) from the WKU Office of Research and Graduate Studies.

References

1 X. Huang and J. T. Groves, *Chem. Rev.*, 2018, **118**, 2491–2553.
2 J. E. Baeckvall, *Modern oxidation methods*, Wiley-VCH Verlag, Weinheim, 2011.
3 T. Punniyamurthy, S. Velusamy and J. Iqbal, *Chem. Rev.*, 2005, **105**, 2329–2363.
4 C. He, J. Cheng, X. Zhang, M. Douthwaite, S. Pattisson and Z. Hao, *Chem. Rev.*, 2019, **119**, 4471–4568.
5 R. A. Sheldon, *Catal. Today*, 2015, **247**, 4–13.
6 *Cytochrome P450 Structure, Mechanism, and Biochemistry*, ed. P. R. Ortiz de Montellano, Kluwer Academic/Plenum, New York, 3rd edn, 2005.
7 I. G. Denisov, T. M. Makris, S. G. Sligar and I. Schlichting, *Chem. Rev.*, 2005, **105**, 2253–2277.
8 B. Meunier, *Chem. Rev.*, 1992, **92**, 1411–1456.
9 R. A. Sheldon, *Metalloprophyrins in Catalytic Oxidations*, Marcel Dekker, New York, 1994.
10 C.-M. Che and J.-S. Huang, *Chem. Commun.*, 2009, 3996–4015.
11 H.-Y. Liu, M. H. R. Mahmood, S.-X. Qiuc and C. K. Chang, *Coord. Chem. Rev.*, 2013, **257**, 1306–1333.
12 *Metal-Oxo and Metal-Peroxo Species in Catalytic Oxidations*, ed. B. Meunier, Springer-Verlag, Berlin, 2000.
13 R. A. Baglia, J. P. T. Zaragoza and D. P. Goldberg, *Chem. Rev.*, 2017, **117**, 13320–13352.
14 J. T. Groves, K. Shalyaev and J. Lee, in *The Porhyrin Handbook*, ed. K. M. S. Kadish and R. Guilard, 2000, vol. 4, pp. 17–40.
15 K. P. Shing, B. Cao, Y. Liu, H. K. Lee, M.-D. Li, D. L. Phillips, X.-Y. Chang and C.-M. Che, *J. Am. Chem. Soc.*, 2018, **140**, 7032–7042.
16 H. Ohtake, T. Higuchi and M. Hirobe, *Heterocycles*, 1995, **40**, 867–903.
17 J. T. Groves, M. Bonchio, T. Carofiglio and K. Shalyaev, *J. Am. Chem. Soc.*, 1996, **118**, 8961–8962.
18 R. Zhang, W.-Y. Yu, K.-Y. Wong and C.-M. Che, *J. Org. Chem.*, 2001, **66**, 8145–8153.
19 A. Petrosyan, R. Hauptmann and J. Pospech, *Eur. J. Org. Chem.*, 2018, 5231–5333.
20 J. T. Groves and R. Quinn, *Inorg. Chem.*, 1984, **23**, 3844–3846.
21 J. T. Groves and R. Quinn, *J. Am. Chem. Soc.*, 1985, **107**, 5790–5792.
22 T.-S. Lai, R. Zhang, K.-K. Cheung, C.-M. Che and H.-L. Kwong, *Chem. Commun.*, 1998, 1583–1584.
23 C.-M. Che, J.-L. Zhang, R. Zhang, J.-S. Huang, T.-S. Lai, W.-M. Tsui, X.-G. Zhou, Z.-Y. Zhou, N. Zhu and C. K. Chang, *Chem. – Eur. J.*, 2005, **11**, 7040–7053.
24 H. Hennig, *Coord. Chem. Rev.*, 1999, **182**, 101–123.
25 D. G. Nocera, *Acc. Chem. Res.*, 2012, **45**, 767–776.
26 D. G. Nocera, *Acc. Chem. Res.*, 2017, **50**, 616–619.
27 R. Zhang, S. Klaine, C. Alcantar and F. Bratcher, *J. Inorg. Biochem.*, 2020, 111246.
28 T.-H. Chen, Z. Yuan, A. Carver and R. Zhang, *Appl. Catal., A*, 2014, **478**, 275–282.
29 X. C. Hu, A. Damjanovic, T. Ritz and K. Schulten, *Proc. Natl. Acad. Sci. U. S. A.*, 1998, **95**, 5935–5941.
30 M. K. Panda, K. Ladomenou and A. G. Coutsolelos, *Coord. Chem. Rev.*, 2012, **256**, 2601–2627.
31 O. Itoa and F. D'Souzab, *ECS J. Solid State Sci. Technol.*, 2013, **2**, 3063–3073.
32 D. Holten, D. F. Bocian and J. Lindsey, *Acc. Chem. Res.*, 2002, **35**, 57–69.
33 A. Loudet and K. Burgess, *Chem. Rev.*, 2007, **107**, 4891–4932.
34 M. T. Whited, P. J. Djurovich, S. T. Roberts, A. C. Durrell, C. W. Schlenker, S. E. Bradforth and M. E. Thompson, *J. Am. Chem. Soc.*, 2011, **133**, 88–96.
35 T. K. Khan, M. Broering, S. Mathur and M. Ravikanth, *Coord. Chem. Rev.*, 2013, **257**, 2348–2387.
36 F. R. Li, S. I. Yang, Y. Z. Ciringh, J. Seth, C. H. Martin, D. L. Singh, D. H. Kim, R. R. Birge, D. F. Bocian, D. Holten and J. S. Lindsey, *J. Am. Chem. Soc.*, 1998, **120**, 10001–10017.

37 F. D'Souza, P. M. Smith, M. E. Zandler, A. L. McCarty, M. Itou, Y. Araki and O. Ito, *J. Am. Chem. Soc.*, 2004, **126**, 7898–7907.

38 M. Koepf, A. Trabolsi, M. Elhabiri, J. A. Wytko, D. Paul, A. M. Albrecht-Gary and J. Weiss, *Org. Lett.*, 2005, **7**, 1279–1282.

39 J. Li, J. R. Diers, J. Seth, S. I. Yang, D. F. Bocian, D. Holten and J. S. Lindsey, *J. Org. Chem.*, 1999, **64**, 9090–9100.

40 M. D. Weber, V. Nikolaou, J. E. Wittmann, A. Nikolaou, P. A. Angaridis, G. Charalambidis, C. K. Stangel, A. G. Coutsolelos and R. D. Costa, *Chem. Commun.*, 2016, **52**, 1602–1605.

41 Q. Miao, J. Y. Shin, B. O. Patrick and D. Dolphin, *Chem. Commun.*, 2009, 2541–2543.

42 A. D. Adler, F. R. Longo, J. D. Finarelli, D. Goldmacher, J. Assour and L. Korsakoff, *J. Org. Chem.*, 1967, **32**, 476.

43 J. Lindsey and R. D. Wagner, *J. Org. Chem.*, 1989, **54**, 828–836.

44 C.-M. Che and W.-Y. Yu, *Pure Appl. Chem.*, 1999, **71**, 281–288.

45 J. Y. Liu, H.-S. Yeung, W. Xu, X. Li and D. K. P. Ng, *Org. Lett.*, 2008, **10**, 5421–5424.

46 N. J. Turro, *Modern Molecular Photochemistry*, University Science Books, Brand, 1991.

47 M. Hoshino and Y. Kashiwagi, *J. Phys. Chem.*, 1990, **94**, 673–678.

48 K. Ishii, S. Hoshino and N. Kobayashi, *Inorg. Chem.*, 2004, **43**, 7969–7971.

49 R. Zhang, W.-Y. Yu, T.-S. Lai and C.-M. Che, *Chem. Commun.*, 1999, 409–410.

50 R. Zhang, W.-Y. Yu, T.-S. Lai and C.-M. Che, *Chem. Commun.*, 1999, 1791–1792.

51 K. W. Kwong, T. H. Chen, W. Luo, H. Jeddi and R. Zhang, *Inorg. Chim. Acta*, 2015, **430**, 176–183.

52 W. H. Leung and C. M. Che, *J. Am. Chem. Soc.*, 1989, **111**, 8812–8818.

53 R. Zhang, W.-Y. Yu, H.-Z. Sun, W.-S. Liu and C.-M. Che, *Chem. – Eur. J.*, 2002, **8**, 2495–2507.

54 T.-H. Chen, K.-W. Kwong, A. Carver, W. L. Luo and R. Zhang, *Appl. Catal., A*, 2015, **497**, 121–126.

55 T. H. Chen, K. W. Kwong, N. G. Lee, D. Ranburger and R. Zhang, *Inorg. Chem. Acta*, 2016, **451**, 65–72.

56 D. Ranburger, B. Willis, B. Kash, H. Jeddi, C. Alcantar and R. Zhang, *Inorg. Chim. Acta*, 2019, **487**, 41–49.